Man-Dominated Landscapes, R. L. Burgess and D. M. Sharpe, Eds. (Springer-Verlag, New York, 1981), pp. 125–205; D. S. Wilcove, *Ecology* **66**, 1211 (1985); ———, C. H. McLellan, A. P. Dobson, in *Conservation Biology: The Science of Scarcity and Diversity*, M. E. Soulé, Ed. (Sinauer, Sunderland, MA, 1986), pp. 237–256; D. S. Wilcove and S. K. Robinson, in *Biogeography and Ecology of Forest Bird Communities*, A. Keast, Ed. (SPB, The Hague, Netherlands, 1990), pp. 319–331; R. A. Askins, J. F. Lynch, R. Greenberg, in *Current Ornithology*, D. M. Power, Ed. (Plenum, New York, 1990), vol. 7, chap. 1; J. Faaborg, M. C. Brittingham, T. Donovan, J. Blake, in (*2*), pp. 331–338.
6. J. E. Gates and L. W. Gysel, *Ecology* **59**, 871 (1978).
7. S. A. Temple and J. R. Cary, *Conserv. Biol.* **2**, 340 (1988).
8. S. K. Robinson *et al.*, in (*2*), pp. 93–102.
9. T. M. Donovan, F. R. Thompson, J. Faaborg, in *Ecology and Management of Cowbirds*, T. Cook, S. K. Robinson, S. I. Rothstein, S. G. Sealy, J. N. M. Smith, Eds. (Univ. of Texas Press, Austin, TX, in press).
10. F. R. Thompson III, S. K. Robinson, T. M. Donovan, J. Faaborg, D. R. Whitehead, in (*9*).
11. S. K. Robinson, in (*1*), pp. 408–418; J. D. Brawn and S. K. Robinson, *Ecology*, in press.
12. H. R. Pulliam, *Am. Nat.* **132**, 652 (1988).
13. P. W. C. Paton, *Conserv. Biol.* **8**, 17 (1994).
14. R. H. Yahner and A. L. Wright, *J. Wildl. Manage.* **49**, 508 (1985); H. Andrén and P. Angelstam, *Ecology* **69**, 544 (1988); M. F. Small and M. L. Hunter, *Oecologia* **76**, 62 (1988); J. T. Ratti and K. P. Reese, *J. Wildl. Manage.* **52**, 484 (1988); H. Andrén, *Ecology* **73**, 794 (1992).
15. J. J. Roper, *Oikos* **65**, 528 (1992).
16. G. G. Chasko and J. E. Gates, *Wildl. Monogr.* **82**, 1 (1982).
17. M. C. Brittingham and S. A. Temple, *BioScience* **33**, 31 (1983).
18. H. Mayfield, *Wilson Bull.* **87**, 456 (1975). The Mayfield index measures the daily predation rate by division of the number of depredated nests by the total number of "exposure days" during which the nests were active and being monitored. Nest predation rates in excess of 5% translate to overall losses of 70% or more of all nests. We accumulated more than 40,000 exposure days for the nine study species.
19. Study areas included northwestern Illinois (NWIL), five woodlots (90 to 525 ha) (1992–1993 only) in Jo Daviess and Carroll counties; central Illinois (CNIL), three woodlots (65 to 300 ha) in Shelby, Champaign, and Piatt counties; southwestern Illinois (SWIL), four areas in 1000- to 3500-ha tracts in the Shawnee National Forest and Trail of Tears State Forest in Union and Alexander counties; Cache River, IL (CAIL), six study sites in 25- to 1600-ha forests in the Cache River Bioreserve of Johnson, Union, Pulaski, and Alexander counties; southern Indiana (SOIN), four study sites (ranging from 133 to 190 ha) in a >40,000-ha forest tract in the vicinity of the Pleasant Run Unit of Hoosier National Forest of Monroe, Brown, Jackson, and Lawrence counties; northwestern Wisconsin (NWWI), six study areas within the Chequamegan National Forest, Bayfield County; west-central Wisconsin (WCWI), six study areas (80- to 160-ha patch size) along the St. Croix River in Washington and Chisago counties, MN, and Polk County, WI; south-central Missouri (SCMO), eight study areas within the contiguous Ozark Forests in Shannon, Reynolds, and Carter counties; north-central Missouri (NCMO), nine study sites within Boone, Callaway, and Randolph counties in tracts ranging from 150 to 900 ha.
20. Study species included the acadian flycatcher (ACFL) *Empidonax virescens*, wood thrush (WOTH) *Hylocichla mustelina*, red-eyed vireo (REVI) *Vireo olivaceus*, ovenbird (OVEN) *Seiurus aurocapillus*, worm-eating warbler (WEWA) *Helmitheros vermivorus*, Kentucky warbler (KEWA) *Oporornis formosus*, scarlet tanager (SCTA) *Piranga olivacea*, northern cardinal (NOCA) *Cardinalis cardinalis*, and indigo bunting (INBU) *Passerina cyanea*. Sample sizes per species ranged from 50 nests (SCTA) to over 500 (ACFL and WOTH).
21. The overlays are available from the U.S. Geological Survey, 507 National Center, Reston, VA 22092.
22. FRAGSTATS; Forest Science Department, Oregon State University, Corvallis, OR.
23. R. R. Sokal and F. J. Rohlf, *Biometry* (Freeman, New York, 1981).
24. R. M. May and S. K. Robinson, *Am. Nat.* **126**, 475 (1985).
25. J. P. Hoover and M. C. Brittingham, *Wilson Bull.* **105**, 228 (1993).
26. S. I. Rothstein, J. Verner, E. Stevens, *Ecology* **65**, 77 (1984); F. R. Thompson III, *Auk*, in press.
27. J. R. Bider, *Ecol. Monogr.* **38**, 269 (1968).
28. T. M. Donovan, thesis, University of Missouri.
29. J. P. Gibbs and J. Faaborg, *Conserv. Biol.* **4**, 193 (1990); M. A. Villard, P. R. Martin, C. G. Drummond, *Auk* **110**, 759 (1993); P. Porneluzi, J. C. Bednarz, L. J. Goodrich, N. Zawada, J. P. Hoover, *Conserv. Biol.* **7**, 618 (1993).
30. For source-sink models of the wood thrush and ovenbird in this landscape, see T. M. Donovan, R. H. Lamberson, F. M. Thompson III, J. Faaborg, *Conserv. Biol.*, in press; T. M. Donovan, F. R. Thompson III, J. Faaborg, J. Probst, *ibid.*, in press.
31. M. A. Van Horn, R. M. Gentry, J. Faaborg, *Auk*, in press.
32. We would like to thank the many assistants who made this project possible, especially the following: in Illinois, S. Morse, S. Bailey, R. Jack, K. Bruner, J. Hoover, C. Morse, S. Daniels, and R. Brumfield; in Missouri, R. Clawson and P. Porneluzi; in Wisconsin, J. Porath and A. R. Weisbrod; and in Indiana, G. Greenberg, M. Koukol, D. Winslow, T. Ford, P. Doran, C. Wilson, B. Geils, and B. Slusher. We also thank D. Larsen and W. Dijak for assistance with the landscape analyses and graphics. J. D. Brawn kindly provided data from two woodlots in CNIL. Funding was provided by the Illinois Departments of Energy and Natural Resources and Conservation (NWIL and SWIL), the National Fish and Wildlife Foundation (SWIL, SOIN, and SCMO), the U.S. Forest Service, North Central Forest Experiment Station (SWIL, NCMO, WCWI, and NWWI), the Illinois Chapter of The Nature Conservancy (CAIL), the U.S. Army Construction Engineering Research Laboratory (CNIL), the Indiana Department of Natural Resources (SOIN), the Martin Foundation (SOIN), the David G. Frey Memorial Fund (SOIN), the Conservation and Research Foundation, Wild Birds Unlimited, the Indiana Academy of Science (SOIN), many Audubon chapters (SOIN), Minnesota Department of Natural Resources Nongame Wildlife Research Fund (WCWI), Missouri Department of Conservation (SCMO), and the Global Change Program (BBIRD) of the National Biological Service (NCMO and SCMO).

24 October 1994; accepted 30 January 1995

Requirement of Serine Phosphorylation for Formation of STAT-Promoter Complexes

Xiaokui Zhang, John Blenis, Heng-Chun Li, Chris Schindler, Selina Chen-Kiang*

Members of the interleukin-6 family of cytokines bind to and activate receptors that contain a common subunit, gp130. This leads to the activation of Stat3 and Stat1, two cytoplasmic signal transducers and activators of transcription (STATs), by tyrosine phosphorylation. Serine phosphorylation of Stat3 was constitutive and was enhanced by signaling through gp130. In cells of lymphoid and neuronal origins, inhibition of serine phosphorylation prevented the formation of complexes of DNA with Stat3-Stat3 but not with Stat3-Stat1 or Stat1-Stat1 dimers. In vitro serine dephosphorylation of Stat3 also inhibited DNA binding of Stat3-Stat3. The requirement of serine phosphorylation for Stat3-Stat3·DNA complex formation was inversely correlated with the affinity of Stat3-Stat3 for the binding site. Thus, serine phosphorylation appears to enhance or to be required for the formation of stable Stat3-Stat3·DNA complexes.

The Janus kinase (Jak)–STAT pathway transduces the signals of many cytokines and peptide growth factors (*1*). Ligand binding rapidly triggers tyrosine phosphorylation of STATs (*2*, *3*) by receptor-associated Jak family tyrosine kinases (*4*, *5*). The activated STATs dimerize and translocate into the nucleus, where they directly activate target genes by binding to specific promoter sequences (*1*). The pleiotropic cytokines interleukin-6 (IL-6), ciliary neurotrophic factor (CNTF), leukemia inhibitory factor (LIF), oncostatin M, and IL-11 transduce signals through gp130, a common component of the receptor complexes (*6*, *7*). IL-6 primarily activates Stat3 [also known as acute-phase response factor (APRF)] (*8*, *9*) in the liver (*9*, *10*), but it also activates Stat1 (*11*) in human hepatoblastoma HepG2 cells (*8*, *12*, *13*). Signaling by CNTF activates Stat1 and two Stat1-related proteins in a human neuroblastoma cell line SK-N-MC (*14*). Activated Stat3 and Stat1 form three distinct protein-DNA complexes that contain either Stat1 homodimers, Stat1-Stat3 heterodimers, or Stat3 homodimers when they bind to the Stat-binding site present in the c-*fos* promoter (*8*, *12*, *13*, *15*). Studies of the activation of Stat1 by interferon γ (IFN-γ) suggest that Stat1 can form stable dimers by interactions between the Src homology 2

X. Zhang and S. Chen-Kiang, Brookdale Center for Molecular Biology, Mount Sinai School of Medicine, New York, NY 10029, USA.
J. Blenis, Department of Cell Biology, Harvard Medical School, Boston, MA 02115, USA.
H.-C. Li, Department of Biochemistry, Mount Sinai School of Medicine, New York, NY 10029, USA.
C. Schindler, Department of Medicine, College of Physicians and Surgeons, Columbia University, New York, NY 10032, USA.
*To whom correspondence should be addressed.

(SH2) domain of one Stat1 protein and the phosphotyrosine of the other protein before translocating into the nucleus (*16*). These interactions are also thought to occur between Stat1 and Stat3.

The activation of STATs is transient (*1*). To investigate the temporal activation of STATs by IL-6, we examined the formation of STAT-DNA complexes in nuclear extracts of IL-6–treated human NJBC T cells, which express a large amount of the IL-6 receptor (*17*), by electrophoretic mobility-shift assays (EMSAs). The STAT-binding site [IFN-γ activation site (GAS)] of the *IRF-1* gene promoter (*18*) was used as a probe (Fig. 1). The slowest migrating protein-DNA complex, complex A, was formed within 1 min of exposure of the cells to IL-6. Complex A contained Stat3 but not Stat1, as indicated by a supershift with an antibody specific for Stat3 (*8*) but not with an antibody specific for Stat1α (*3*). The formation of complex A was followed by the formation of a complex of intermediate mobility, complex B, which contained both Stat3 and Stat1. Finally, after 12 min, the fastest migrating complex, complex C, which contained Stat1 but not Stat3, was formed. The DNA binding activities of STATs declined within 2 hours after activation. Within this period of time, the formation of complex A was rapid and more sustained, whereas the formation of complex C was delayed and more transient. Similar kinetics for STAT-DNA complex formation was observed in human B lymphoblastoid CESS cells and mouse myeloid leukemia M1 cells in response to IL-6 (Fig. 1A) (*19*). The sequential formation of protein-DNA complexes differing in the composition of Stat3 and Stat1 indicates that IL-6 preferentially activates Stat3, but it can also activate Stat1 in a time-dependent manner.

Treatment of SK-N-MC cells and human Ewing sarcoma EW-1 cells of neuronal origin (6) with CNTF led to the formation of the three protein-DNA complexes in the same order. However, in contrast to the predominant presence of complex A in IL-6 signaling, the ratios between the three complexes changed rapidly (within 5 min) to favor complex C in CNTF-treated cells (Fig. 1B) (*19*). Thus, although the order of Stat3 and Stat1 activation was similar, the assembly or the stability of STAT-DNA complexes was different in response to IL-6 or CNTF.

We next used confocal immunocytochemistry to examine the subcellular distribution of Stat3 and Stat1 in response to IL-6. Cells were simultaneously stained for Stat3 and a cytoplasmic marker, glucose-regulated protein 94 (GRP94) (*19*), or for Stat1 and GRP94 (Fig. 2). Stat3 was distributed diffusely in both the cytoplasm and

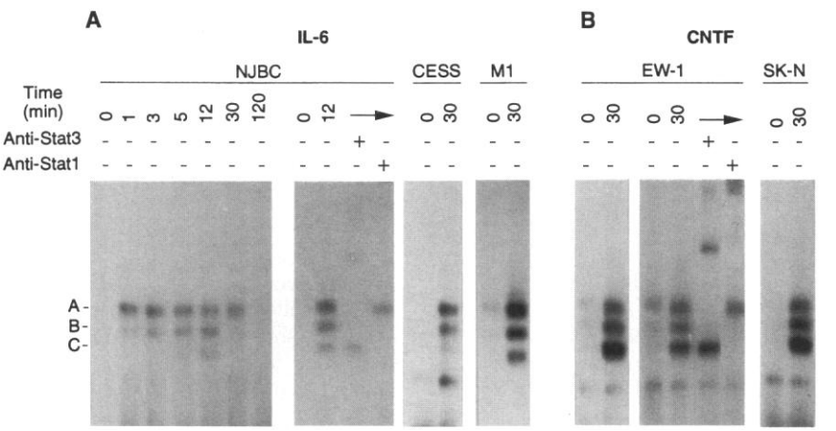

Fig. 1. Kinetic analysis of the activation of Stat3 and Stat1 by IL-6 and CNTF. (**A**) Nuclear extracts were prepared from untreated (0) or IL-6–treated NJBC (120 U/ml), CESS (40 U/ml), and M1 (200 U/ml) cells (*17, 28*) for the time indicated (*2*). EMSA was performed (*2*) with a double-stranded oligonucleotide probe containing the GAS site of the *IRF-1* gene (5′-GATCGATTTCCCCGAAAT-3′). The STATs present in the protein-DNA complexes were identified with rabbit antisera to either the COOH-terminus of Stat3 (anti-Stat3) (*8*) or the COOH-terminal 36 amino acids of Stat1α (anti-Stat1) (*3*). The three protein-DNA complexes formed (named A, B, and C) were separated from free probes by electrophoresis on a 4.5% polyacrylamide gel. (**B**) Nuclear extracts were prepared from EW-1 and SK-N-MC (SK-N) cells left untreated (0) or treated with CNTF (50 ng/ml, Regeneron) (*6*) for the time indicated, and the extracts were analyzed as in (A).

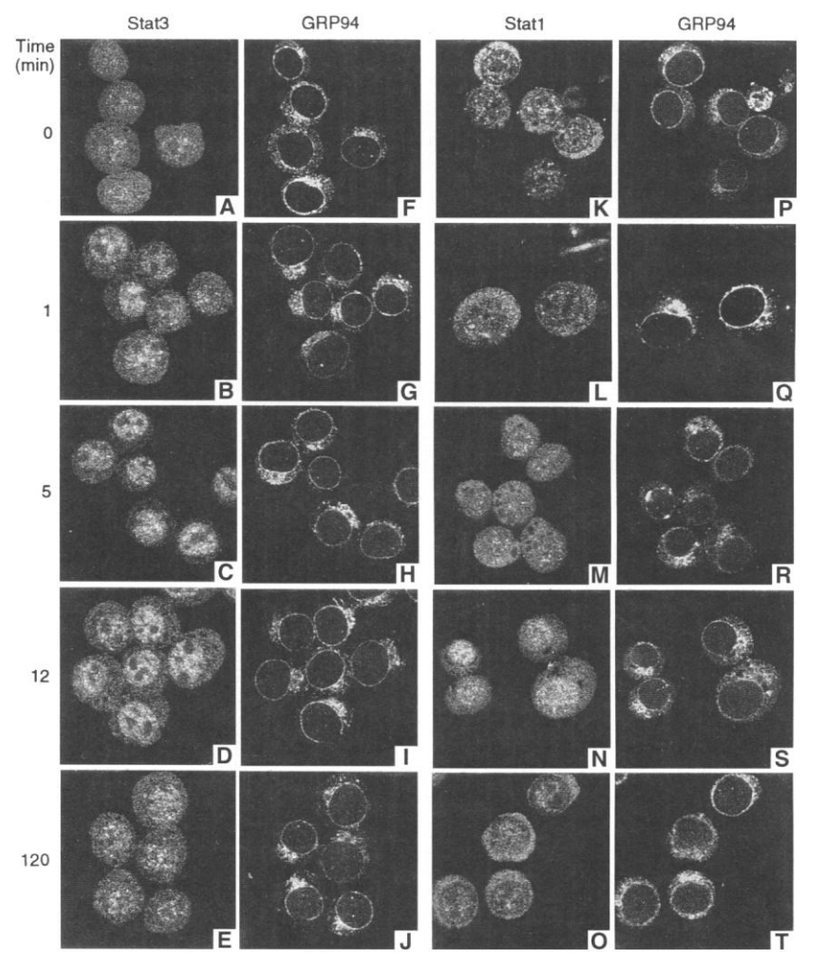

Fig. 2. Differential nuclear localization of Stat3 and Stat1 induced by IL-6. NJBC cells were incubated in the absence (0) or presence of IL-6 for the indicated time, double-stained for Stat3 (**A** through **E**) and GRP94 (**F** through **J**; Stressgen, Victoria, British Columbia, Canada), or for Stat1 (**K** through **O**) and GRP94 (**P** through **T**), and analyzed by confocal microscopy (*2, 19*). Original magnification, ×1000.

the nucleus of untreated NJBC cells, as compared with the restricted endoplasmic reticulum distribution of GRP94. Within 1 min of IL-6 binding and coincidental with the formation of Stat3-Stat3·DNA complexes (Fig. 1), Stat3 was preferentially localized in the nucleus. By 12 min, Stat3 was distributed mainly in the nucleus with a punctate appearance, but not in the nucleoli. Stat3 remained primarily in the nucleus even after its DNA binding activity had declined, whereas GRP94 was always confined to the endoplasmic reticulum.

Stat1 was predominantly present in the cytoplasm of untreated NJBC cells and did not translocate into the nucleus until 5 min after treatment of the cells with IL-6 (Fig. 2). By 12 min, the translocated Stat1 was distributed diffusely in the nucleus. However, unlike Stat3, Stat1 reappeared in the cytoplasm after its DNA binding activity declined. Thus, Stat3 and Stat1 differ in their subcellular distribution, their kinetics of nuclear translocation, and their fate after cells are activated with IL-6. The orderly formation of Stat3-Stat3, Stat3-Stat1, and Stat1-Stat1 protein-DNA complexes in the nucleus of IL-6–treated cells appears to be at least in part the result of sequential nuclear translocation of activated Stat3 and Stat1.

The rapid nuclear translocation of Stat3 suggested that IL-6 rapidly induces phosphorylation of Stat3 on tyrosine. Proteins in Stat3 immune complexes recovered from nuclear extracts of IL-6–treated NJBC cells were probed with an antibody to phosphotyrosine (anti-pTyr). Two proteins that migrated at 88 and 89 kD were rapidly phosphorylated after IL-6 binding (Fig. 3). Both were Stat3, as shown by stripping and probing the same blot with an antibody to Stat3. Referred to as $Stat3_s$ (for slower migrating) and $Stat3_f$ (for faster migrating), they are likely to be the two Stat3 proteins previously identified (*14*, *20*). Consistent with immunocytochemical analysis (Fig. 2), small amounts of both types of Stat3 proteins were present in the nuclear extracts of untreated cells (Fig. 3). However, they were not phosphorylated on tyrosine until the cells were treated with IL-6, which preferentially enhanced the accumulation of $Stat3_s$. Probing of the same blot simultaneously with antibodies to Stat3 and Stat1 showed that, concurrent with time-dependent formation of the Stat3-Stat1·DNA complex (Fig. 1), Stat1 coprecipitated with Stat3 in increasing amounts. The rapid nuclear translocation of Stat3 (Fig. 2) and formation of Stat3-Stat3·DNA complexes (Fig. 1) therefore correlated with rapid tyrosine phosphorylation of Stat3 proteins.

The presence of two Stat3 proteins derived from one mRNA species (*8*, *9*) that were both phosphorylated on tyrosine (Fig. 3) suggested that Stat3 underwent additional posttranslational modification. Serine-threonine phosphorylation has been implicated in gp130 signaling because activation of immediate early gene transcription by IL-6 and LIF was inhibited by the serine-threonine kinase inhibitor H7 (*21*). H7 also inhibited INF-γ–dependent activation of transcription of the gene encoding GBP, a guanylate-binding protein (*22*). Because the STAT-binding site is present in the promoters of the *Fos*, *JunB*, and *GBP* genes (*12*, *14*, *19*, *23*), we reasoned that serine-threonine phosphorylation might function in the activation of STATs, or the formation of STAT-promoter complexes.

Treatment of NJBC cells with H7 before stimulation with IL-6 prevented the formation of the Stat3-Stat3·DNA complex (complex A), but not that of Stat3-Stat1· (complex B) or Stat1-Stat1·DNA complex (complex C), when the GAS site was used as a probe in EMSA (Fig. 4A). The broad-spectrum kinase inhibitor staurosporine abolished the formation of all three complexes in vivo, presumably because it inhibited tyrosine phosphorylation. These results indicated that serine-threonine phosphorylation was specifically required for the formation of stable Stat3-Stat3·DNA complexes in vivo. In vitro dephosphorylation of IL-6–induced nuclear extracts with the serine-threonine–specific phosphoprotein phosphatase 2A (PP2A) selectively inhibited Stat3-Stat3 complex formation in a concentration-dependent manner. PP2A is

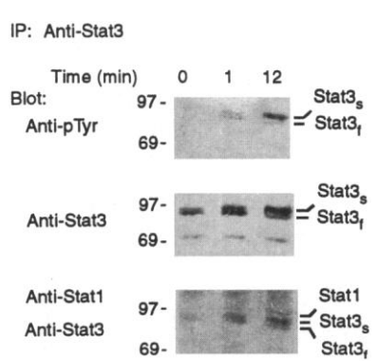

Fig. 3. IL-6–induced tyrosine phosphorylation of two Stat3 proteins. NJBC cells were left untreated (0) or treated with IL-6 for 1 or 12 min. Proteins from nuclear extracts were immunoprecipitated with anti-Stat3 and analyzed by immunoblotting (*2*) sequentially with a monoclonal antibody to phosphotyrosine (anti-pTyr) (4G10, Upstate Biotechnology, 1:1000), anti-Stat3 (1:1000), and both anti-Stat3 and anti-Stat1 (1:1000). The bound antibodies were detected by using an epichemiluminescence immunoblotting system (Amersham). $Stat3_s$ and $Stat3_f$ indicate the migrations of the two Stat3 proteins. At left are prestained protein size markers in kilodaltons.

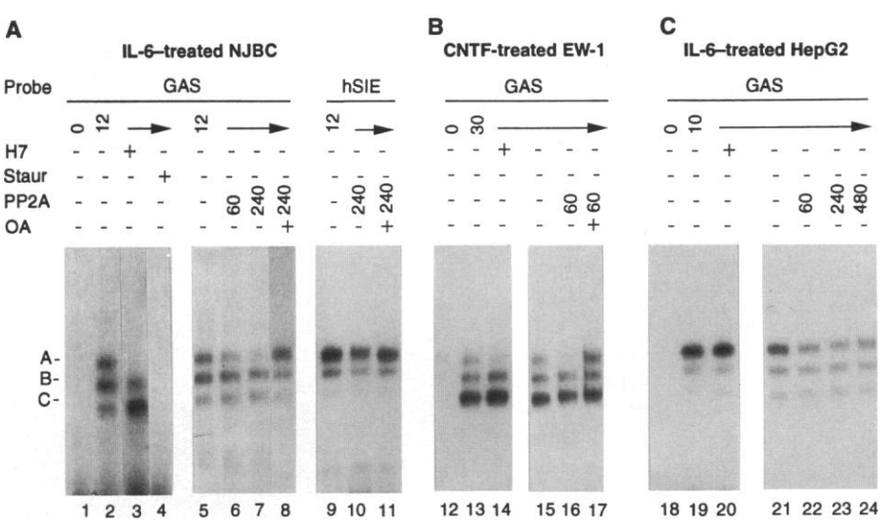

Fig. 4. Inhibition of STAT-DNA complex formation by kinase inhibitors and serine-threonine dephosphorylation. (**A**) Nuclear extracts were prepared from NJBC cells left untreated (0) or treated with IL-6 for 12 min. H7 (50 μM, Seikagaku, Rockville, Maryland) or staurosporine (staur) (500 nM, Sigma) was added (+) to selected cultures for 1 hour before cytokine treatment (lanes 3 and 4). The 12-min nuclear extracts were incubated with PP2A purified from bovine brain at the concentrations indicated (units × 10^{-3}) in the presence of KCl (50 mM) and $MnCl_2$ (1 mM) for 10 min at room temperature (*29*), without (lanes 5 to 7) or with okadaic acid (OA) (50 nM, Sigma) (lane 8). The subsequent formation of STAT-DNA complexes was analyzed by EMSA with the GAS site probe (lanes 1 to 8) or the hSIE probe (double-stranded GTCGACATTTCCCGTAAATCGTCGA) (*12*) (lanes 9 to 11). (**B**) Nuclear extracts were prepared from EW-1 cells left untreated (0) or treated with CNTF for 30 min in the absence or presence of H7 (lanes 12 to 14). The CNTF-treated nuclear extracts were incubated with PP2A in the absence (lane 16) or presence of okadaic acid (50 nM) (lane 17). (**C**) Nuclear extracts were prepared from HepG2 cells left untreated (0) or treated with IL-6 for 10 min in the absence or presence of H7 (lanes 18 to 20). The IL-6–treated nuclear extracts were incubated with PP2A as indicated (lanes 21 to 25). Complexes A, B, and C are indicated at the left.

a dominant protein phosphatase in vivo and can be inhibited by okadaic acid (*24*). Co-incubation of PP2A with okadaic acid completely protected the Stat3-Stat3·DNA complex from PP2A activity.

To address the possibility that serine-threonine phosphorylation may be required for stable Stat3-Stat3·DNA complex formation in a site-specific manner, we used the STAT-binding site of the *Ly-6E* gene promoter (Ly-6E) (*25*), which binds Stat3-Stat3 with relatively lower affinity (*19*), and a high-affinity sis-inducible element of the c-*fos* promoter (hSIE) (*12, 15*) as probes in EMSAs (Fig. 4A). Although dephosphorylation of Stat3 with PP2A also abolished the binding of Stat3-Stat3 to Ly-6E (*19*), it only marginally affected (20%) binding to hSIE. The requirement of serine-threonine phosphorylation for the formation of stable Stat3-Stat3·DNA complexes therefore appeared to be inversely correlated with the affinity between the Stat3-Stat3 homodimer and its binding site.

The formation of the Stat3-Stat3·DNA complex at the GAS site was similarly reduced in EW-1 cells by either H7 treatment of the cells before stimulation with CNTF or dephosphorylation of proteins in vitro with PP2A (Fig. 4B). The inhibitory effect of H7 appeared to be cell type–dependent, because formation of Stat3-Stat3·DNA complexes in response to IL-6 was not sensitive to inhibition by H7 in some cells such as HepG2 (Fig. 4C) (*20*). However, treatment of nuclear extracts from IL-6–activated HepG2 cells with PP2A decreased, but did not eliminate, the formation of Stat3-Stat3·DNA complexes (Fig. 4C). Thus, inhibition of serine-threonine phosphorylation by H7 in vivo prevented the formation of Stat3-Stat3·DNA complexes in a cell type–dependent manner. In vitro dephosphorylation by PP2A mimicked the H7 effect, even in nuclear extracts of cells that were not sensitive to inhibition by H7. Therefore, serine-threonine phosphorylation appears to enhance or be required for the formation of Stat3-Stat3·DNA complexes in certain cells.

To further investigate the role of serine and threonine phosphorylation in the formation of Stat3-Stat3·DNA complexes, we performed a phosphoamino acid analysis of Stat3 (Fig. 5). Stat3 was immunoprecipitated from lysates of untreated and IL-6–treated NJBC cells labeled with [^{32}P] orthophosphoric acid. The incorporation of ^{32}P into Stat3 was increased fourfold in response to IL-6 (Fig. 5A). Phosphoamino acid analysis showed that Stat3 was not appreciably phosphorylated on tyrosine until it was activated by IL-6. Tyrosine phosphorylation then increased more than 35-fold (Fig. 5B). In contrast, serine phosphorylation of Stat3 was constitutive, representing 90% of the total ^{32}P incorporated into Stat3 in untreated cells. In response to IL-6, serine phosphorylation of Stat3 was increased fourfold, which accounted for most of the total increases in ^{32}P incorporated into Stat3.

Because dephosphorylation with PP2A did not affect the formation of Stat3-Stat1· and Stat1-Stat1·DNA complexes (Fig. 4), selective inhibition of Stat3-Stat3·DNA complex formation was probably the result of dephosphorylation on serine and not on tyrosine. Phosphotyrosine on Stat3 was retained after dephosphorylation with PP2A, as shown by anti-pTyr blotting of Stat3 isolated from the same CNTF-induced EW-1 cell nuclear extracts used in the EMSAs (Figs. 4B and 5C). Thus, serine phosphorylation of Stat3 is constitutive and enhanced by IL-6 signaling, and removal of the phosphate group or groups from serine correlates with inhibition of Stat3-Stat3·DNA complex formation.

In summary, in addition to tyrosine phosphorylation, serine phosphorylation has a function in the Jak-STAT pathway. Specifically, it enhanced or was required for the formation of stable Stat3-Stat3·DNA complexes in a cell type– and site-dependent manner. In contrast to the detailed understanding of the function of tyrosine phosphorylation in the Jak-STAT pathway and the mechanism involved, very little is known about serine phosphorylation in this pathway. Comparison of Stat3 and Stat1, which also appears to be constitutively phosphorylated on serine residues contained in two or three tryptic peptides (*3, 5, 26*), suggests that serine phosphorylation on Stat3 may also be limited to specific residues. The sequence -Pro-Met-Ser-Pro-, which resembles the consensus sequence for the mitogen-activated protein (MAP) kinase substrate -Pro-X-Ser (Thr)-Pro- (*27*), is present in the conserved region in the COOH-terminus of Stat1, Stat3, and Stat4. Thus, it is possible that the Jak-STAT pathway may be functionally coupled to and modulated by the MAP-kinase pathway.

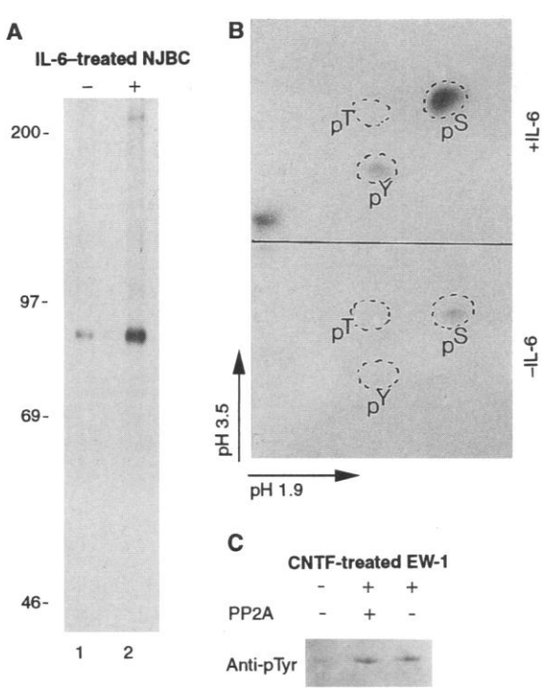

Fig. 5. Serine phosphorylation on Stat3 is constitutive and enhanced by IL-6. (**A**) NJBC cells (4×10^7) were biosynthetically labeled with carrier-free [^{32}P] orthophosphoric acid (500 μCi/ml, DuPont-NEN) for 2 hours and either left untreated (–) or treated with IL-6 for 10 min (+). The proteins in cell lysates were immunoprecipitated with anti-Stat3 and resolved by SDS–polyacrylamide gel electrophoresis on a 7.5% gel as described (*30*). At left are prestained protein size markers in kilodaltons. (**B**) Phosphoamino acid analysis of Stat3. The ^{32}P-labeled Stat3 was recovered from the gel shown in (A) and analyzed for the presence of phosphoamino acids by two-dimensional thin-layer electrophoresis, with the first dimension performed in pH 1.9 buffer and the second dimension performed in pH 3.5 buffer (*30*). The labeled phosphoamino acids (pS, phosphoserine; pT, phosphothreonine; pY, phosphotyrosine) were quantified by phosphoimager analysis. (**C**) The nuclear extracts of EW-1 cells used in EMSA (Fig. 4) were analyzed by immunoblotting with anti-pTyr.

REFERENCES AND NOTES

1. J. E. Darnell Jr., I. M. Kerr, G. R. Stark, *Science* **264**, 1415 (1994).
2. C. Schindler, K. Shuai, V. R. Prezioso, J. E. Darnell Jr., *ibid.* **257**, 809 (1992).
3. K. Shuai, C. Schindler, V. R. Prezioso, J. E. Darnell Jr., *ibid.* **258**, 1808 (1992).
4. N. Stahl *et al.*, *ibid.* **263**, 92 (1994); K. Shuai *et al.*, *Nature* **366**, 580 (1993).
5. C. Lütticken *et al.*, *Science* **263**, 89 (1994).
6. N. Y. Ip *et al.*, *Cell* **69**, 1121 (1992).
7. T. Kishimoto, T. Taga, S. Akira, *ibid.* **76**, 253 (1994).
8. Z. Zhong, Z. Wen, J. E. Darnell Jr., *Science* **264**, 95 (1994).
9. S. Akira *et al.*, *Cell* **77**, 63 (1994).
10. U. M. Wegenka, J. Buschmann, C. Luttichen, P. C. Heinrich, F. Horn, *Mol. Cell. Biol.* **13**, 276 (1993).
11. C. Schindler, X.-Y. Fu, T. Improta, R. Aebersold, J. E. Darnell Jr., *Proc. Natl. Acad. Sci. U.S.A.* **89**, 7836 (1992).
12. H. B. Sadowski, K. Shuai, J. E. Darnell Jr., M. Z. Gilman, *Science* **261**, 1739 (1993).
13. P. Rothman *et al.*, *Immunity* **1**, 457 (1994).
14. A. Bonni, D. A. Frank, C. Schindler, M. E. Greenberg, *Science* **262**, 1575 (1993).
15. B. J. Wagner, T. E. Hayes, C. J. Hoban, B. H. Cochran, *EMBO J.* **9**, 4477 (1990).
16. K. Shuai *et al.*, *Cell* **76**, 821 (1994).

17. W. Hsu and S. Chen-Kiang, *Mol. Cell. Biol.* **13**, 2515 (1993).
18. R. Pine, C. Schindler, A. Canova, *EMBO J.* **13**, 158 (1994).
19. X. Zhang, D. Chen, S. Chen-Kiang, in preparation.
20. U. M. Wegenka *et al.*, *Mol. Cell. Biol.* **14**, 3186 (1994).
21. K. Nakajima and R. Wall, *ibid.* **11**, 1409 (1991); K. A. Lord *et al.*, *ibid.*, p. 4371.
22. D. J. Lew, T. Decker, J. E. Darnell Jr., *ibid.* **9**, 5404 (1989).
23. T. Decker, D. J. Lew, J. Mirkovitch, J. E. Darnell Jr., *EMBO J.* **10**, 927 (1991).
24. T. A. J. Haystead *et al.*, *Nature* **337**, 78 (1989).
25. K. D. Khan *et al.*, *Proc. Natl. Acad. Sci. U.S.A.* **90**, 6806 (1993).
26. O. Silvennoinen, C. Schindler, J. Schlessinger, D. E. Levy, *Science* **261**, 1736 (1993); S. Ruff-Jamison, K. Chen, S. Cohen, *ibid.*, p. 1733.
27. E. Alvarez *et al.*, *J. Biol. Chem.* **266**, 15277 (1991).
28. Y. Natkunam, X. Zhang, Z. Liu, S. Chen-Kiang, *J. Immunol.* **153**, 3476 (1994).
29. H.-C. Li and W. S. Chan, *Arch. Biochem. Biophys.* **207**, 270 (1981).
30. R.-H. Chen and J. Blenis, *Mol. Cell. Biol.* **10**, 3204 (1990).

31. We thank J. E. Darnell Jr., T. Roberts, and W. Yokoyama for critical comments and encouragement; Z. Zhong for discussions and rabbit antisera to Stat3; G. Yancopoulus for discussions and CNTF; L. May for an IL-6 expression vector; V. Frederick, A. Fannon, and L. Morse for advice on immunocytochemistry and confocal microscopy; and L. Morse and Q. Ye for photography. Supported by grants to J.B. from NIH (CA46595), to C.S. from NIH (HL 21006), and to S.C.-K. from the American Cancer Society (IM548).

16 November 1994; accepted 23 February 1995

Switching Recognition of Two tRNA Synthetases with an Amino Acid Swap in a Designed Peptide

Douglas S. Auld and Paul Schimmel

The genetic code is based on specific interactions between transfer RNA (tRNA) synthetases and their cognate tRNAs. The anticodons for methionine and isoleucine tRNAs differ by a single nucleotide, and changing this nucleotide in an isoleucine tRNA is sufficient to change aminoacylation specificity to methionine. Results of combinatorial mutagenesis of an anticodon-binding–helix loop peptide were used to design a hybrid sequence composed of amino acid residues from methionyl- and isoleucyl-tRNA synthetases. When the hybrid sequence was transplanted into isoleucyl-tRNA synthetase, active enzyme was generated in vivo and in vitro. The transplanted peptide did not confer function to methionyl-tRNA synthetase, but the substitution of a single amino acid within the transplanted peptide conferred methionylation and prevented isoleucylation. Thus, the swap of a single amino acid in the transplanted peptide switches specificity between anticodons that differ by one nucleotide.

Isoleucyl- and methionyl-tRNA synthetases are two of the most closely related class I tRNA synthetases (*1*). Each has a characteristic nucleotide binding fold in the NH_2-terminal domain that forms the active site for amino acid activation and for the transfer of the activated amino acid to the bound tRNA. A polypeptide insertion into this domain is believed to provide for interaction with the tRNA acceptor helix (*2*). The COOH-terminal domain is rich in α helices and provides for interaction with the anticodon of the respective tRNAs. Within this second domain, a helix loop peptide provides for interactions with the anticodon. Chemical crosslinking, molecular modeling, and mutagenesis have implicated Trp^{461} (*3*) of the peptide element of *Escherichia coli* methionyl-tRNA synthetase (MetRS) as essential for this anticodon interaction (Fig. 1) (*4–9*). In particular, Trp^{461} is proposed to interact with the first base cytosine of the CAU anticodon of $tRNA^{Met}$ (*10*). Sequence alignments show that in *E. coli* isoleucyl-tRNA synthetase (IleRS), the analogous position is Arg^{734} (Fig. 1).

Muramatsu *et al.* (*11*) further demonstrated the relatedness of these enzymes by the ease with which their respective tRNA specificities could be switched. Although the minor isoacceptor of $tRNA^{Ile}$ has an LAU anticodon, where L is lysidine (lysidine is cytosine with the ε-amino group of lysine covalently linked to C-2 of the pyrimidine ring of cytosine), the unmodified isoacceptor has a CAU anticodon—the same as $tRNA^{Met}$. This unmodified $tRNA^{Ile}$ is aminoacylated efficiently by MetRS but not by IleRS. Modification of C → L yields efficient aminoacylation with isoleucine and eliminates aminoacylation with methionine. We sought to determine whether a complement of the experiment performed by Muramatsu *et al.* could be achieved by manipulation of the two enzymes. Our initial experiments concentrated on gathering more information about the role of 10 amino acids within the helix loop element that includes Arg^{734} of IleRS and Trp^{461} of MetRS (Fig. 1).

Synthetic deoxyoligonucleotide cassettes that encode variants of the helix loop peptide were introduced into plasmids pKSNB (which encodes MetRS) and pDUG03 (which encodes IleRS) through unique restriction sites (*12*). The genes that encode

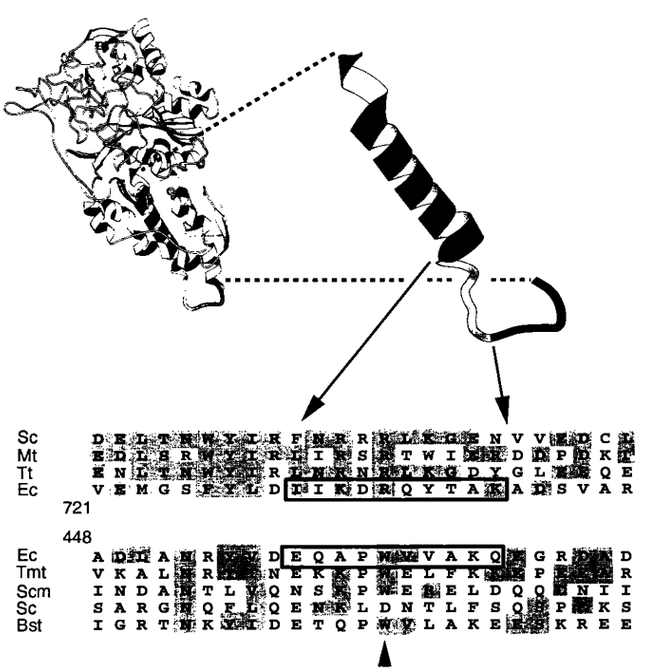

Fig. 1. (Top) The helix loop structure derived from the crystal structure of the 547–amino acid monomeric fragment of MetRS (*5*); the fragment was drawn with the program Molscript (*29*). (Bottom) A portion of the alignment used to define the anticodon-binding region in IleRS (upper four sequences) and MetRS (*3, 13, 20, 30*). Also shown is the 10–amino acid region that was combined (boxed residues) by binary codon mutagenesis (*18*). Shaded regions represent semiconserved residues in IleRS sequences that also are semiconserved in MetRS sequences. The arrowhead at the bottom points to the anticodon recognition region. Ec, *E. coli*; Sc, *Saccharomyces cerevisiae*; Mt, *Methanobacterium thermoautotrophicum*; Tt, *Tetrahymena thermophila*; Tmt, *Thermus thermophilus*; Scm, mitochondrial *Saccharomyces cerevisiae*; and Bst, *Bacillus stearothermophilus*.

Department of Biology, Massachusetts Institute of Technology, Cambridge, MA 02139, USA.